Journal of Solar Energy Research (JSER)

Journal homepage: jser.ut.ac.ir

Design and Implementation of a Hybrid Fuzzy Logic Controller with Thermal Energy Storage System for Reference Power Tracking in a Large-Scale Solar Chimney Power Plant

Amir Arefian, Reza Hosseini Abardeh*

Mechanical Engineering Department, Amirkabir University of Technology (Tehran Polytechnic), Tehran, Iran.

Abstract

Solar Chimney Power Plant (SCPP) is known as a relatively new technology for electrical power generation from solar thermal energy in a relatively simple structure and reliable operation. SCPP would be one of the main competitors with traditional power generation technol ogies for the present time and near future. Considering the variable nature of solar radiation and ambient temperature during a day and different days of a year as the main plant's excitation factors, it is essential to control the power output of solar chimney power plant to meet the various demands of local and national electrical grids. The design and implementation of a Fuzzy Logic Control (FLC) system for a large-scale solar chimney power plant equipped with natural or artificial thermal storage to meet various base to peak demand patterns studied in this paper. The power error between actual power generation and the reference value and the rate of change in that error are defined as the controller inputs. A knowledge base of IF-THEN rules is generated based on expert knowledge and the dynamic behaviour of the plant. The output of the controller, the opening of the turbine inlet gate, will impose on the plant. Simulation results show that SCPPs equipped with an integrated active and passive control system, including FLC and thermal energy storage, can track daily reference profiles in various grid demand patterns and different ambient conditions.

Keywords: Solar Chimney Power Plant; Active and Passive Control; Fuzzy Logic Control; Thermal Energy Storage; Electrical Grid Demand.

1. Introduction

Increasing global demand for electricity and the presence of limitations and some problems due to the use of fossil fuels requires greater use of renewable energy resources. Among the renewable energies, the most abundant energy resource available to human society is solar energy. The energy received by the earth and its atmosphere at 4×10^6 EJ/year is ten thousand times the energy consumption of the world in 2007 [1]. There are many technologies and methods to harvest solar energy and convert it to the desired form in various applications like power generation, heating, cooling, food drying, and desalination.

Solar Chimney Power Plant (SCPP) is a relatively new and one of the most efficient technologies for electrical power generation on a large scale [2]. Significant advantages of this technology include simplicity of the structure, reliable operation, and low relative investment and maintenance costs. Also, the availability of the construction materials in sufficient

* *Department of Mechanical Engineering, Amirkabir University of Technology (Tehran Polytechnic), 424 Hafez Ave, P. O. Box 15875-4413 Tehran-Iran, Tel.: +98 21 64543433, fax: +98 21 66419736, Email address: hoseinir@aut.ac.ir (R.Hosseini)*

quantities in a wide range of regions, continuous operation with low cost natural or artificial thermal storage, without the need for cooling water, no pollutant emission should be added to these advantages [3]. SCPP is one of the cleanest power generation options for the current and future world electricity generation.

The Solar chimney power plant comprises three main components: solar collector or greenhouse, Power Conversion Unit (PCU), and chimney. The air in the collector warms up by greenhouse effect, and updraft flow will produce due to buoyancy and chimney effect; thermal energy of the air converts to kinetic energy that can drive a turbo-generator and generate electricity. Natural soil or water volume in dark bags or closed tubes at the bottom of the solar collector can act as natural or artificial thermal storage to absorb solar radiation in the day time and release it to flowing air at night time or cloudy conditions. A schematic of the configuration and operation of a typical solar chimney power plant is shown in Fig. 1.

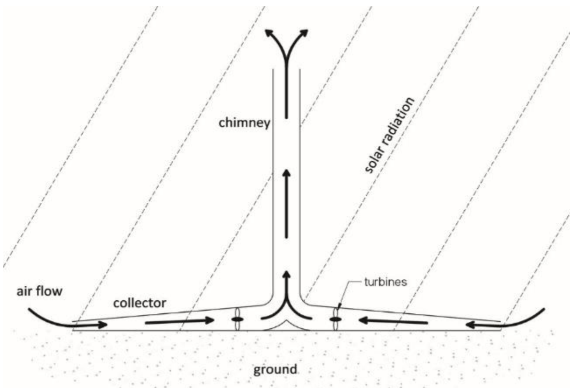

Figure 1. Schematic of configuration and operation of a typical SCPP [4]

Cabanyes first introduced harvesting energy from the hot rising air in the solar chimney configuration in 1903; after that, Dubas proposed the construction of a solar chimney in the north of Africa in 1926 [5]. In 1931 Gunther described some aspect of this technology, and finally, the first pilot plant of solar chimney technology was designed and constructed by Schlaich and his partners in Manzanares, Spain (1982). This SCPP prototype has a chimney with 195 m in height and 10 m in diameter, a solar collector with 46000 m^2 in area, and about 2 m height from the ground. The peak power output from the Manzanares project was 50 kW, and it was operating between 1982 to 1989 [4].

Various experimental models have been built and tested by researchers creating the opportunity for comparison between experimental and numerical or analytical results. Determination of conducive weather conditions and site selection, experimental determination of the temperature field in the solar collector, effect of environmental condition change as well as geometrical parameters on system performance and study of night operation of the plant are some aspects of consideration [6-10]. Some researchers investigated the analysis of the airflow and heat transfer in these systems and proposed some methods for optimizing solar chimney geometry and increasing output electrical power and overall efficiency [11-16]. Kebasa et al. [17] performed a numerical analysis on a sloped solar collector integrated with a chimney and a PCU. The results verified with experimental data show that an SCPP with an appropriate collector slope can produce more power about 16% greater than a conventional zero-sloped solar collector. A comparison between the performance of an SCCP with and without a thermal energy storage (TES) system is carried out by Yaswanthkumar and Chandramohan [18] at steady-state conditions. 3D numerical analysis shows that by the implementation of a TES system, the main flow parameters, including velocity, pressure, and temperature, will decrease due to the storing of heat energy in storage. Referring to the steady-state analysis, it is not possible to study the effect of the TES system on the time-depended performance of an SCCP. Similar results were obtained in a 3D-numerical analysis presented by Amudam and Chandramohan [19]. Muhammed and Atrooshi [20] developed a mathematical model for a solar chimney power plant with the aim of geometrical optimization. The diameter of the solar collector was selected as an independent parameter, and 180 cases are run to obtain optimal values to other geometrical dimensions. Numerical optimization results show the there is a semi-linear relation between chimney height, chimney diameter, and collector height with collector diameter. Mehla et al. [21] studied the effect of various absorbers in the solar collector of an SCPP experimentally. Black resin plastic, gray sand, water packets, and small pieces of stone were used in their research as absorbers bed. Analysis of results on the collector efficiency, chimney efficiency, and overall efficiency show that implementation of small stone pieces causes lead to more overall and partial efficiencies in the system, but no further discussions are provided for time-averaged efficiencies in daily or seasonal operation. Fallah and Valipour [22] evaluated the effect of artificial roughness at the solar collector bed. The results of a three-dimensional simulation reveal that although heat transfer is improved, the flow rate is reduced when artificial roughness is applied; So, there is an optimal for dimension and location for the added roughness. Das and Chandramohan [23, 24] performed a computational study by using ANSYS® Fluent® on the effect of collector cover inclination angle, collector diameter, and chimney height on the plant's flow parameters. Results show that chimney height has a significant effect on the flow velocity and power output compared with the other parameters. Cottam et al. [25] conducted a detailed study on the plant dimensioning for optimal operation. A semi-analytical thermodynamic model was used to identify the key parameters that drive performance. One of the main results was that the dependency of turbine optimum pressure ratio on collector and chimney diameters, while other geometrical and environmental were not effective. Based on thermo-economical calculations, they recommended using several plants with small collectors and chimneys instead of one massive plant for the same power generation. Bouabidi et al. [26] studied the effect of solar chimney diameter on the performance of an SCCP based on experimental and numerical analysis. They found that the updraft velocity and efficiency of the plant will increase with increasing chimney diameter. Balijepalli et al. [27] developed an analytical model to evaluate the design and performance parameters on an SCCP. They focused on solar radiation calculations, chimney design, aero-turbine design calculations, and heat and pressure losses in the solar collector. Al-Kayiem et al. [28] and Aurybi et al. [29] introduced and evaluated a hybrid solar chimney power plant for uninterrupted power generation. In their study, besides the solar energy used in the collector, flue-gas from industrial plants as an external source is utilized to boost the collector air heating and continuously the SCCP operation during night time. Zhou and Xu [30] investigated a detailed mathematical model to calculate all components of pressure drop in a solar chimney power plant. Their study shows that the exit dynamic pressure drop at the chimney outlet is dominant in the system, and other pressure losses have a small portion, and collector inlet loss is negligible. In the following of the previous paper, Xu and Zhou [31] studied the performance of divergent-chimney solar power plants to reduce the effect of exit dynamic pressure drop. Results show that the total pressure potential, updraft mass flow rate, and power output will increase and reach their maximum values when the degree of divergence increases. After that, the main flow parameters will reduce due to the boundary layer separation and cold ambient air backflow to the chimney. Another study on the plant geometrical optimization, especially about divergence chimney, was performed by Hassan et al. [32]. They used the discrete ordinate (DO) model for solar load and RNG k-ε turbulent model for simulating the fluid flow. Based on computed results, diverging the chimney has a significant effect on the induced flow in the system. Also, increasing the slope angle of the solar collector causes an increase in inside velocity and temperature while deteriorate the smooth flow by generating the vortices and recirculating flow at higher collector slope; Thus, there was an optimum value for the slope angle. Three-Dimensional Numerical simulations were performed by Toghraie et al. [33] to investigate the effects of the geometrical parameters on the performance of the plant. They demonstrate that the chimney height has a significant effect on the output power, while the collector diameter has a small effect. On the other hand, the diameter of the chimney has an optimum range to maximize the chimney efficiency and plant output. Rabehi et al. [34] performed a full 3D numerical simulation with considering the turbine based on the fan model. They considered a constant value for turbine pressure drop in each case from 40 to 220 Pa and independent of flow velocity. Results show that by increasing the turbine pressure drop, the flow velocity will decrease, and while the temperature and pressure inside the collector will increase. The effect of turbine pressure drop on the collector efficiency reported ineffective while it is significant on the output power. Djaouida et al. [35] performed a numerical study on controlling the output power of an SCCP referring to grid demand. They evaluated the impact of the secondary and tertiary roof under the main roof in the collector proposed by Pretorius [36] for satisfying the baseload electricity generation. Balijepalli et al. [37] estimated the optimized design and performance parameters for a small scale of wind turbines uses in an SCPP. Schmitz theory and aerodynamics forces are used to determine the optimal values for pitch angle, relative wind angle, lift force, and relative chord length. Ayadi et al. [38] performed a numerical simulation for the unsteady operation of a solar chimney power plant coupled with an aero-turbine. Multiple Reference Frame (MRF) model was implemented to simulate the presence of the turbine. Zhou et al. [39] developed a one-dimensional steady-state mathematical model to study the effect of flow area and turbine pressure drop factor on the performance of an SCCP. Constant density and variable density for working flue were evaluated in this study, and obtained results reveal that for the first assumption optimal turbine pressure drop factor is equal to 2/3 and for the second assumption will close to 1 while effected by the flow area parameters. Divergent-top chimney and sloped-to-center solar chimney are recommended to better performance of an SCPP. Ming et al. [40] performed a case study on a novel type of solar collector with radial partition walls. They show that the new collector design can eliminate the negative effect of ambient crosswind on the system by reducing the flow mixing inside the collector and heated flow escaping to the ambient. Li et al. [41] analyzed one of the most crucial characteristics of SCPPs, power generation quality, and performed optimization. They introduced some correlations between geometrical parameters such as chimney height, collector diameter, chimney diameter, and thermal storage thickness to operate the plant in optimal power quality factor and stabilized power generation. Guo et al. [42] proposed a detailed analytical approach to evaluate the optimal turbine pressure drop factor by using m-th power-law assumption. In the following, a 3D numerical simulation was used to investigate the effect of different values for m. Numerical results show that the m value significantly depends on solar radiation and ambient temperature; as a result, the optimum value of the turbine pressure drop factor will not be constant at different conditions. They found that the optimal values vary from 0.90 to 0.94 for the Manzanares pilot under normal climate conditions. Choi et al. [43] developed an analytical model for predicting the time-depended operation of a solar chimney power plant with and without water bags as thermal energy storage. The results show that by increasing water storage thickness, the peak value of output power will be passed to the end hours of the day, while the maximum output power will be decreased and make a smooth power generation curve. A similar trend was observed for both small and large scale of the SCPPs.

Based on the literature survey presented above, several studies are found on plant geometrical optimization, fluid flow, and heat transfer analysis in steady-state operation. Also, the determination of an optimal value for turbine pressure drop, and the implementation of thermal energy storage as a passive control solution have been under investigation. There is no particular study found on active control of an SCPP power generation. Global solar radiation (beam and diffuse) and ambient temperature are the main factors affecting the operation of the system. Considering their variations during a day and different days of a year implies the use of additional thermal storage in the collector to give a smoother daily profile for generated power and make it possible to operate during night hours and cloudy conditions [2, 5, 11, 14, 44-46]. However, once the thermal storage is implemented, there is no further control of the plant performance. The use of artificial thermal storages like dark water bags or tubes constitutes only a passive control of the system. On the other hand, to meet the different needs of local or national electrical grid demands, active control on power generation is required.

In this research, active control on storing heat and generating electrical energy is done by control of the system flow due to the change of pressure drop in the turbines inlet gate. The energy and momentum equations are coupled together, referring to the dominant process in and SCPP system, which is natural convection. This active control system applies two inputs, power generation error between instantaneous plant generation and its reference value and rate of change of its error. As mentioned earlier, the output of this controller must determine the level of turbine inlet gate opening to maintain the system flow in the desired value. It seems that by using an integrated active and passive control systems in an SCPP, a wide range of demand patterns on the local or national grid can be satisfied. Also, the flexibility of the plant in power generation will be improved reasonably and cost-effectively. It must be noted that some proposed semi-active solutions, such as the implementation of secondary or tertiary collector roof [36], may not be techno-economical feasible on a large scale of a solar power plant.

Due to several advantages of Fuzzy Logic Control (FLC), such as the ability to overcome the system nonlinearities and achieve robustness and simplicity, this approach is used to design and implement a novel SCPP active control system. Fuzzy Logic Control is a methodology to represent and implement a human's knowledge about how to control a system. A flow chart of a fuzzy controller is shown in Fig. 2. Fuzzy controllers provide a heuristic approach to nonlinear control construction [47] and more robustness than conventional types [48]. They are represented by IF-THEN rules and thus can provide a user-friendly and understandable knowledge representation such that in this work. The knowledge base of rules is determined by system behavior and the qualitative perception of SCPP experts. Notably, in the field of renewable technologies and solar energy, FLC has a wide range of interests, such as nonlinear control of parabolic trough solar power plant to obtain desired oil outlet temperature and flow rate [49-51]. Also, the optimization of a solar array performance and control of the sun-tracking systems in photovoltaic applications by the use of FLC systems were studied [52-56].

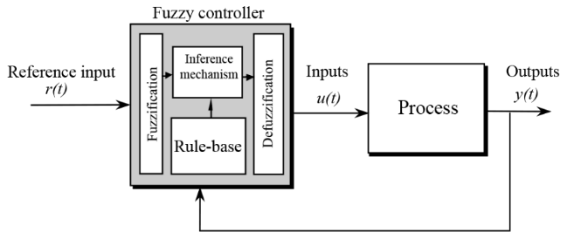

Figure 2. Main Components of a Fuzzy Logic Controller [47]

The main objectives and novelties in this work are summarized in the following:

- Develop a realizable semi-analytical mathematical model for predicting the time-depended operation of an SCCP with the ability to apply active and passive control strategies.
- Propose and design the cost-effective, feasible, and novel type of active control system for SCPPs base on FLC.
- Evaluate the implementation of active, passive, and integrated control solutions on a large-scale SCPP facing fluctuations of solar radiation and ambient temperature to meet different demand patterns.

2. Materials and Methods

2.1. Mathematical Model for an SCPP Dynamic Performance

In this section, a mathematical model for describing the dynamics of an SCPP time-dependent performance is developed based on its thermodynamic cycle. In this analysis, ambient conditions, including ambient temperature, global horizontal irradiation, and local gravitational acceleration, are known. Geometrical parameters of the plant comprise of chimney height, collector diameter, collector height, and chimney radius are predefined.

Due to the radiation properties of the collector, especially ground (as the thermal storage media) absorptivity and the collector roof transmissivity, part of the solar irradiation will be absorbed by the collector and heats the ground and the airflow adjacent to it; thus the governing equation for energy conservation in the solar collector is defined in equation (1).

$$\alpha\tau G_h A_c = h_i A_c\left(T_s - \bar{T}_a\right) + m_s c_s \frac{dT_s}{dt} \qquad (1)$$

where α and τ are the absorptivity of the ground and transmissivity of the collector roof, respectively. G_h is instantaneous global horizontal irradiation and $A_c = \pi D_c^2 / 4$ is the total collector area in a circular configuration. On the right-hand side of equation (1), T_s and $\bar{T}_a$ are the thermal storage (collector ground) temperature and the average temperature of the flowing air, respectively. The effective mass of the thermal storage is $m_s = \rho_s A_c H_s$ where H_s is the effective thickness of the thermal storage and c_s is its specific heat capacity. For the flowing air inside the collector, energy conservation equation is:

$$\begin{aligned} h_i A_c\left(T_s - \bar{T}_a\right) &= \dot{m}_a c_{pa}\left(T_{a_o} - T_{ai}\right) \\ &\quad + h_\infty A_c\left(\bar{T}_a - T_\infty\right) \end{aligned} \qquad (2)$$

Part of the energy transferred from thermal storage heats the flowing air and the rest losses through the collector roof. In equation (2), $\dot{m}_a$, c_{pa}, T_{a_o} and T_{ai} are mass flow rate, specific heat capacity, outlet and inlet temperature of the flowing air inside the collector, respectively. It should be noted that the mean temperature of the air is expressed as $\bar{T}_a = 0.5\left(T_{a_o} + T_{a_i}\right)$. T_∞ is the ambient temperature outside the collector and h_∞ is the external heat transfer coefficient which can be estimated as a function of ambient wind speed with a linear relation [57]:

$$h_\infty = 5.7 + 3.8 u_{wind} \qquad (3)$$

The internal heat transfer coefficient h_i is taken as [58, 59]:

$$h_i = \frac{(f/8)(Re - 1000)Pr}{1 + 12.7\sqrt{f/8}(Pr^{\frac{2}{3}} - 1)} \frac{k}{D_h} \qquad (4)$$

where friction factor f is a function of Reynolds number, $Re = \rho_a \bar{u}_c D_h / \mu_a$ with the relation $f = \left[0.79 \ln(Re) - 1.64\right]^{-2}$ in turbulent flow, and D_h is the hydraulic diameter of the solar collector with the definition of $D_h = 4A_{wet}/p_{wet} = 2H_c$. According to the variation of the radial velocity of the air inside the collector, the mean air radial velocity is calculated by integral averaging of the local velocity through the collector radius [46]:

$$\begin{aligned} \bar{u}_c &= \frac{\dot{m}_a}{2\pi\rho_a\left(R_c - R_t\right)H_c}\int_{R_t}^{R_c}\frac{dr}{r} \\ &= \frac{\dot{m}_a}{2\pi\rho_a\left(R_c - R_t\right)H_c}\ln\frac{R_c}{R_t} \end{aligned} \qquad (5)$$

where ρ_a is the mean air density evaluated at $\bar{T}_a$. R_c and R_t are collector and chimney (tower) radius, respectively.

In the mentioned equations, the main unknown parameters are T_s, T_a and $\dot{m}_a$. Other unknowns like T_{ao} and h_i can be computed by auxiliary equations previously discussed. Besides the two energy equations (1) and (2), another relation is necessary to make a closed-form problem and calculate the main unknowns. In the natural convection process that occurs in the solar chimney power plant, energy and momentum equations are coupled and must be solved at the same time; thus, the final equation to be used is the conservation of momentum in the whole system. Here this equation is defined based on pressure rise and pressure drop terms. The driving force (pressure difference or pressure potential) due to natural draft in the chimney is defined as:

$$\Delta p_{tot} = g\int_0^{H_t}\left(\rho_\infty - \rho_{a,o}\right)dH_t \approx g\left(\rho_\infty - \rho_{a,o}\right)H_t \qquad (6)$$

where Δp_{tot} is the total available pressure difference, $\rho_{a,o}$ is the flowing air density at the base of the chimney that is evaluated at $T_{a,o}$ and H_t is the chimney height. Δp_{tot} will force the inside air to move and finally will be balanced with the summation of the pressure drop in the turbine Δp_t, the pressure drop in turbine inlet gate Δp_g, pressure drop due to minor and major (frictional) losses Δp_l

and dynamic pressure of the flowing air Δp_d at chimney outlet, so that:

$$\Delta p_{tot} = \Delta p_t + \Delta p_g + \Delta p_l + \Delta p_d \qquad (7)$$

By using the standard definition of dynamic pressure:

$$\Delta p_d = \frac{1}{2}\rho_{a,o} v_a^2 \qquad (8)$$

where $\rho_{a,o}$ is the density of flowing air at chimney inlet (collector outlet) and v_a is updraft (vertical or axial) velocity of the flowing air inside the chimney. The whole pressure drop due to frictional and local losses can be estimated by equation (9).

$$\begin{aligned}\Delta p_l &= \frac{1}{2}\sum\left(f_i \frac{L_i}{D_{h,i}} + K_i \right)\rho v^2 \\ &= \xi \frac{1}{2}\rho_{a,o} v_a^2 \approx \xi\,\Delta p_d\end{aligned} \qquad (9)$$

where ξ is the whole pressure coefficient of minor and major losses and its variation can be neglected in typical operating conditions.

Without losing the generality, the pressure drop in the turbine and its inlet gate are modeled as $\Delta p_t = \psi\,\Delta p_{tot}$ and $\Delta p_g = \chi(1-\psi)\Delta p_{tot}$ where ψ and χ are pressure drop coefficients in the turbine and its inlet gate, respectively. These definitions have physical meaning such that in the constant load condition ($\psi = cte$), the value of χ shows the level of the opening of the inlet gate. When $\chi = 0$ the gate is fully opened ($v_a = \sqrt{\frac{2(1-\psi)\Delta p_{tot}}{(1+\xi)\rho_{a,o}}}$) and when $\chi = 1$, the gate is fully closed ($v_a = 0$); thus, all the incident energy will be stored in the thermal storage or lost to the ambient atmosphere in this situation. Therefore χ can be used as the primary control parameter in the SCPP system. As expected, by controlling the momentum transfer in the system (pressure drop in turbine inlet gate or active control on χ), energy transfer and conversion can be controlled in a solar chimney power plant. Finally, the power generation in the plant is calculated by:

$$P = \eta_{tg}\Delta p_t\,\dot{Q}_a = \eta_{tg}\psi\,\Delta p_{tot}\,\frac{\dot{m}_a}{\rho_{a,o}} \qquad (10)$$

where P is the instantaneous generated power of the plant, η_{tg} is the turbo-generator efficiency, and $\dot{Q}_a$ is the volumetric flow rate of the air flowing through the aero-turbine.

2.2. Design of Fuzzy Logic Controller (FLC) System

In order to satisfy local or national grid demand for power generation in an SCPP, an active control system must be used for tracking the desired daily or seasonal power demand profile. The design process and adoption of an FLC system to the plant are presented in this section. There are several design concerns that one encounters when constructing a fuzzy controller. It is generally essential to have a perfect understanding of the control problem, including the plant dynamics and closed-loop specifications [47], as discussed earlier.

The first step in designing a fuzzy logic controller is to determine the inputs and outputs of the controller. Based on the semantic analysis of the present problem, a Multi-Input and Single-Output (MISO) controller can be adequate for all power generation strategies. Instantaneous power generation, as closed-loop system feedback. This fuzzy controller has two inputs, which include the error in power generation (e) and the rate of change in this error (c) where defined in equations (11) and (12).

$$e(nT) = P_r(nT) - P(nT) \qquad (11)$$

$$c(nT) = \frac{e(nT) - e(nT-T)}{T} \qquad (12)$$

P_r is the reference power output determined by electrical grid demand. The output of this fuzzy controller is pressure drop coefficient in turbine inlet gate or similarly, level of inlet gate closing (χ) that should be imposed on the plant. Solar chimney power plant dynamic performance is simulated as a continuous-time system that is controlled by a fuzzy controller that is implemented on a digital computer with a sampling interval time T . The closed-loop of an SCPP control system is shown in Fig. 3. The desired FLC controller structure is similar to the schematic shown in Fig. 2. Input gains g_1 and g_2 should be appropriately tuned. As a rule of thumb, the first guess for these gains can be obtained in the following way [60]: The gain g_1 can be chosen such that the range of values that e typically takes on will not make it saturate the corresponding outermost input membership functions, for example in a 200MW SCPP the range e is in the order of 10^8 Watts and g_1 can be estimated to be 10^{-8} for this situation. The gain g_1 can be determined by experimenting with various inputs to the fuzzy control system to determine the normal range of values that c will take on. Using this, the gain g_2 is selected so that normally encountered values of c will not result in saturation of the outermost input membership functions, in the SCPP control problem this gain will be tuned by trial and error. Finally, g_0 is chosen so that the range of feasible outputs is the maximum possible value and, in the meantime, the input to the plant will not saturate. For present FLC, the gain g_0 will be estimated to be 1, according to the range of $0 \le \chi \le 1$.

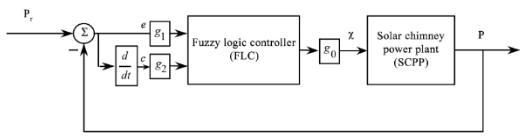

Figure 3. Control system for power generation in a solar chimney power plant

2.2.1. Generating FLC knowledge-base (IF-THEN rules)

Constructing a rule base is one of the most critical steps in the controller design procedure. In this fuzzy controller design, 11 fuzzy sets are defined for each controller input (e and c) such that the membership functions are triangular shaped and evenly distributed on the appropriate universe of discourse. It should be noted that FLC uses the normalized universe of discourse for each input and output, and the controller gains scale the corresponding values from/to plant. The fuzzy sets for the fuzzy controller output are also assumed to be triangular membership functions with a width of 0.4 in the normalized output universe of discourse and centered at zero. Membership functions in the normalized universe of discourse for inputs e and c are shown in Fig. 4.

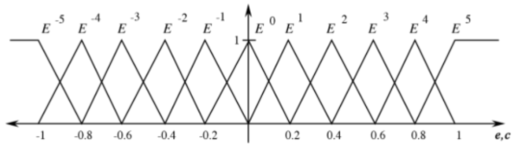

Figure 4. Fuzzy sets (triangular membership functions) for inputs in the normalized universe of discourse

Each membership function is associated with a corresponding linguistic variable. For example, E^5 means positive-very large, E^{-2} means negative-small.

For the FLC output, a new parameter δ is used instead of χ according to the below auxiliary relation:

$$\delta = 2(\chi - 0.5) \; or \; \chi = \frac{\delta}{2} + 0.5 \qquad (13)$$

As a physical interpretation, FLC output determines the new value of the opening gate from 50% of its opening instead of fully closed or fully opened, so that it is expected that the response of control system will increase and the normalized universe of discourse between -1 and +1 can be used for δ parameter to determine the χ in the distance [0,1]. Knowledge-base of FLC is defined based on δ. The degree of gate closing χ will be calculated with equation (13) and will be imposed on the plant. The rule-base for the fuzzy controller has rules of the form:

IF $\tilde{e}$ is $\tilde{E}^j$ and $\tilde{c}$ is $\tilde{C}^l$ THEN $\tilde{\delta}$ is $\tilde{\Delta}^m$

where $\tilde{e}$ and $\tilde{c}$ denote the linguistic variables associated with controller inputs $e(nT)$ and $c(nT)$, respectively, $\tilde{\delta}$ denotes the linguistic variable associated with the controller output δ, $\tilde{E}^j$ and $\tilde{C}^l$ denote the $j^{th}(l^{th})$ linguistic value associated with $\tilde{e}(\tilde{c})$, respectively, and $\tilde{\Delta}^m$ denotes the consequent linguistic value associated with $\tilde{\delta}$. As an example, one fuzzy control rule for the SCPP could be:

IF $\tilde{e}$ is positive-large AND $\tilde{c}$ is negative-small THEN $\tilde{\delta}$ is positive-big

Other rules are generated like the above example, and the knowledge base of IF-THEN rules is presented in Table 1. The center of the output membership function for each rule j and l is named $c_{j,l}$ to emphasize that it is the center associated with the output membership function that has the j^{th} membership function for the $\tilde{e}$ universe of discourse and the l^{th} membership function for the $\tilde{c}$ universe of discourse. Thus, the entries of the table represent the center values of symmetric triangular-shaped membership functions $c_{j,l}$ with base widths 0.4 for output fuzzy sets $\tilde{\Delta}^m$ on the normalized universe of discourse. Notably, the rule-base array shown in Table 1 is employed for the fuzzy inverse model for the solar chimney power plant since information about the plant inverse dynamics is used in its specification [60].

Table 1. Knowledge-Base array for the SCPP fuzzy control system

$c_{j,l}$		C_c^l										
		-5	-4	-3	-2	-1	0	1	2	3	4	5
	-5	1.0	1.0	1.0	1.0	1.0	1.0	0.8	0.6	0.4	0.2	0.0
	-4	1.0	1.0	1.0	1.0	1.0	0.8	0.6	0.4	0.2	0.0	-0.2
	-3	1.0	1.0	1.0	1.0	0.8	0.6	0.4	0.2	0.0	-0.2	-0.4
	-2	1.0	1.0	1.0	0.8	0.6	0.4	0.2	0.0	-0.2	-0.4	-0.6
	-1	1.0	1.0	0.8	0.6	0.4	0.2	0.0	-0.2	-0.4	-0.6	-0.8
E_e^j	0	1.0	0.8	0.6	0.4	0.2	0.0	-0.2	-0.4	-0.6	-0.8	-1.0
	1	0.8	0.6	0.4	0.2	0.0	-0.2	-0.4	-0.6	-0.8	-1.0	-1.0
	2	0.6	0.4	0.2	0.0	-0.2	-0.4	-0.6	-0.8	-1.0	-1.0	-1.0
	3	0.4	0.2	0.0	-0.2	-0.4	-0.6	-0.8	-1.0	-1.0	-1.0	-1.0
	4	0.2	0.0	-0.2	-0.4	-0.6	-0.8	-1.0	-1.0	-1.0	-1.0	-1.0
	5	0.0	-0.2	-0.4	-0.6	-0.8	-1.0	-1.0	-1.0	-1.0	-1.0	-1.0

2.2.2. Fuzzification, Inference Mechanism, and Defuzzification

Fuzzification is the process of transforming the numeric inputs into a form that can be used by the inference mechanism. In the SCPP control system fuzzification part, for the given fuzzy controller inputs e and c, the certainty is determined, and their associated membership functions will be generated. The inference mechanism uses information about the current inputs (formed by fuzzification), decides which rules to apply in the current situation, and forms conclusions about what the plant input should be. For the SCPP control system, the inference mechanism uses the Mamdani method based on Zadeh (min-max) operators [48] to infer and aggregate output fuzzy sets. Defuzzification converts the conclusions reached by the inference mechanism into a numeric input for the plant. Here, to determine the crisp value for δ (and calculate the value of χ in equation (13) to impose to the plant) center of gravity (COG) method is used for defuzzification [48].

2.3. Numerical Method

The governing equations described in section 2.1, make a Differential-Algebraic Equations (DAE) system consisting of one 1st-order ODE and multiple algebraic equations. All equations in that system are coupled and non-linear and must be solved in each time step simultaneously. For the algebraic part of this DAE, a modified fixed-point iteration method is used to calculate algebraic unknowns like mass flow rate of flowing air, the mean temperature of the air. The initial guess for the mentioned parameters is obtained from their values in the previous time step. This approach can accelerate the converging process and reduce noise and disturbance in the numerical solution. Converging criteria for iteration method used in the algebraic part is determined 10^{-6} for all residuals. Differential part of the DAE is solved by the 4th-order Runge-Kutta method. It is considering that there is a single differential variable T_s in the DAE, and its initial condition is set to a temperature a little more than ambient temperature. Notably, the simulation time is selected so that the effect of the initial condition is thoroughly damped, and the plant operates under the excitation of the variation of solar radiation only. The time step used in the differential part is set to 5 seconds in all cases. It differs from sampling interval time T at which the controller takes samples from the plant output and, if required, outputs a new value of the controller output. To ensure that there is enough time to change the turbine inlet gate position by a respective mechanism, sampling interval time is set to $T = 15$ seconds. For simulating with/without the control system, a MATLAB® code is developed. Results are validated, and implementation of FLC in a large scale 200MW solar chimney power plant will be discussed in the next section.

3. Results & Discussion

The results of plant simulation and implementation of the designed FLC are presented in the current section. First, the simulation code is validated, and reference results (plant without any active control system) are obtained. Feasibility study and numerical simulation of a 200MW solar chimney power plant have been investigated by some researchers [2, 5, 61]. In order to validate and compare the results with available resources, the geometrical characteristics of a 200MW SCPP and typical ambient conditions of the plant site are obtained from Hammadi [46] work that listed in Table 2.

Table 2. Geometrical characteristics of the SCPP and ambient conditions [46]

Parameters	Value	Unit
Chimney (tower) height	1000	m
Chimney diameter	100	m
Solar collector diameter	5000	m
Collector height	3	m
Thermal storage height (water tube or bag)	5	cm
Ambient wind velocity	3	m/s
Ambient temperature	25	ºC
Day length	12	hour
Thermal storage absorptivity	0.9	-

The maximum solar radiation is assumed to be 1000 W/m^2, and the daily profile of solar radiation is modeled by $G_h(t) = 1000\sin\left(\frac{\pi t}{\Gamma}\right)$ where t is the time from sunrise and Γ is day length defined in Table 2 [46].

3.1. Code Validation and Reference Results

Validation of simulation code without any control system is shown in Fig. 5. In order to show the effect of thermal storage (in this case, 5 cm in thickness for water tubes or bags) in storing the thermal energy and creating time lag in plant response, the profile of global solar irradiation is shown on the right axis of all output power plots. As can be seen, there is good conformity between present simulation results and data obtained from [46], and thus the code can be accepted as validated one. The output power generation curve in this figure will be used as the output power of the reference plant, and control strategies are applied to this by using the designed FLC system. Another point of consideration is that the natural or artificial thermal storages can damp a considerable variation in solar radiation and make output power smoother, as well as create a significant lag in the plant response such that an SCPP can continue its power generation for a finite time after sunset. Anyhow, modification in a TES process is not possible due to a constructed plant regarding the passive control system. Finally, as shown in Fig. 5, the daily power output of the SCPP has a wide variation from about 0 Watts at the end of night hours to 200MW at midday. The electrical grid management will not accept this output power profile, and thus the power plant requires massive and high-cost mechanical and electrical instruments to deliver produced power to the grid in suitable power quality characteristics, especially regarding the frequency. One of the main advantages of the active control on an SCPP power plant is to satisfy power quantity in a simple and acceptable cost manner.

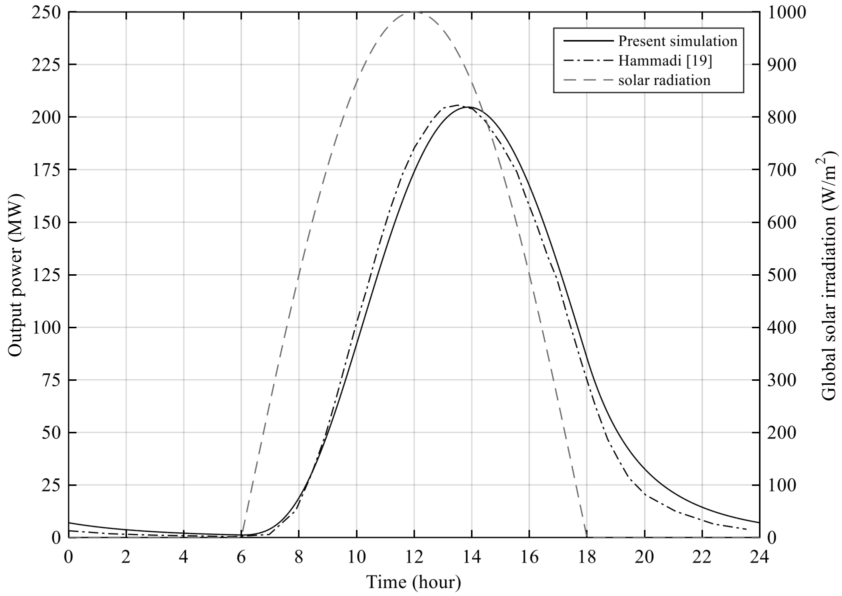

Figure 5. Validation of simulation code and presentation of reference daily power generation profile

3.2. SCPP Active Control for Base Load Demand Pattern

In this section, active control is applied to SCPP power generation by executing the designed fuzzy logic control system. Traditional power generators like steam and gas turbine power plants can produce power in nearly constant values all the time; thus, they are base load power stations and can satisfy required power demand according to their constant capacity. In order to evaluate the FLC performance interacting with an SCPP, it is assumed that grid demand is base load generation (the constant output power, for the longest possible time during a day). In this scenario, reference power applied to the FLC system has a constant value. Fig. 6 shows the results for the implementation of the fuzzy logic controller in order to supply constant power in a base load power generation scenario.

The FLC system can control output power in the desired period that SCPP can produce electrical power above that desired value. The comparison between three case studies done for 150, 100 and 50 MW base load power generation with the output power of the reference SCPP, shows that active control on the plant can make it a base load generator by storing more solar energy in the form of heat in thermal storage and improve power generation at night time. It is expected that with enhancement in heat capacity of the thermal storage (for example increasing the water storage thickness), constant power generation will be available for a long time after sunset. However, base load scenario and power generation with appropriate quality can be obtained in a day time with the designed fuzzy control system. Controller inputs and output in the case of reference output power 50 MW are shown in Fig. 7. A suitable tuning of the scaling gains is done, so there is no saturation condition, and the overshoot and delay are within a reasonable range. Finally, the non-linear mapping between FLC inputs and output is shown in Fig. 8, which is conventionally called controller surface.

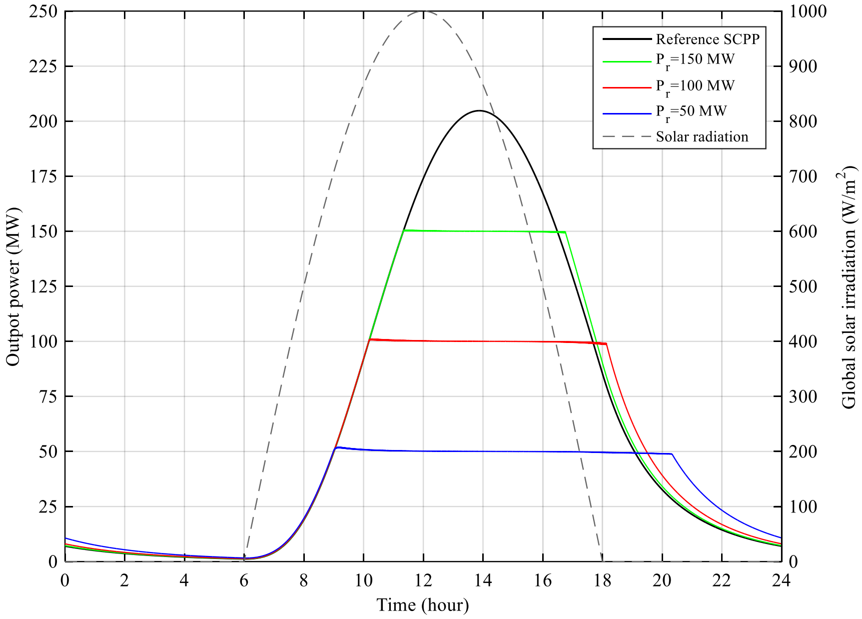

Figure 6. Implementation of Fuzzy control system on a 200MW SCPP for base load generation

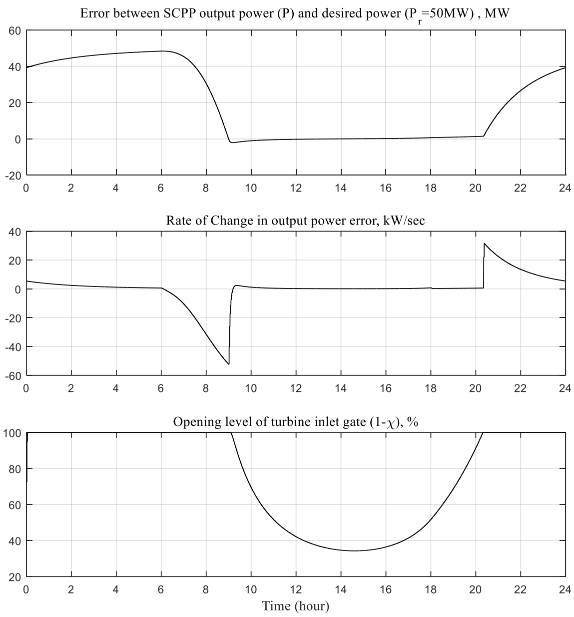

Figure 7. Values of FLC controller inputs and output in base load (50MW) scenario

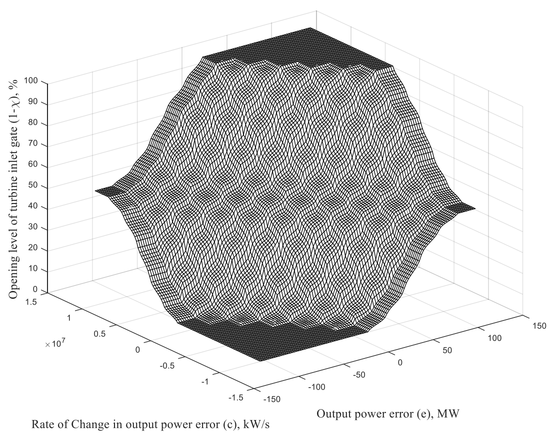

Figure 8. Fuzzy controller mapping between inputs and output

3.3. SCPP Active Control for Peak Load Demand Pattern

Another scenario that is of interest in this work is to apply the designed FLC system on the solar chimney power plant for peak shaving in the national electrical grid. In many countries, peak load demand exists from the beginning of the night (sunset) to about four hours later. This subsection aims to show that SCPPS equipped with FLC systems and thermal energy storage can solve the peak load demand problem satisfactorily. In order to simulate this condition, a reference power P_r is applied to the controller system. It is assumed that peak load demand occurs in a region where solar radiation follows the curve shown in Fig. 5. The reference power profile has a trapezoidal shape, which increases from 1MW to 100MW between hours 17:00 to 18:00 and returns to its minimum value between hours 22:00 to 23:00. In this case, SCPP must produce 100MW power for four hours continuously. The simulation results of this scenario are shown in Fig. 9.

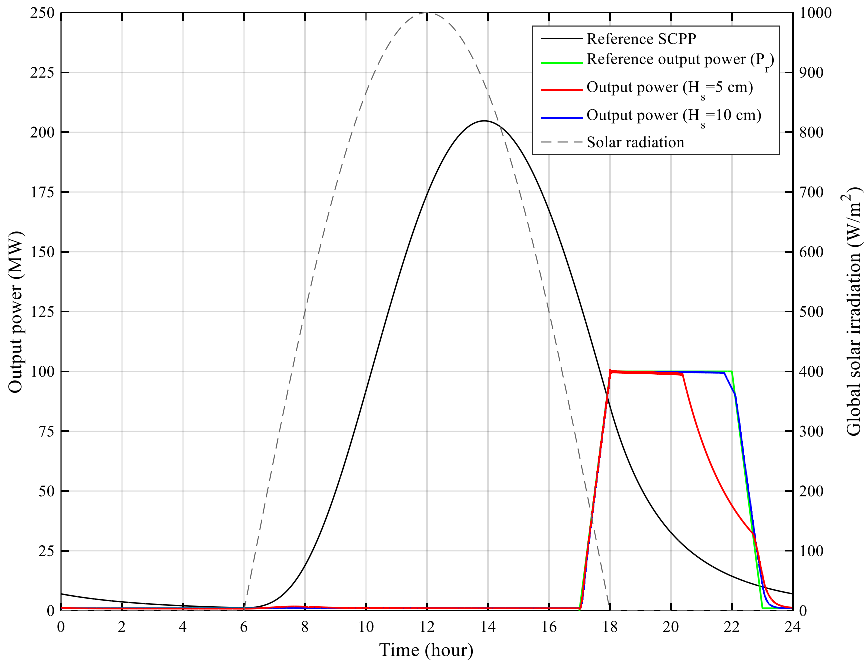

Figure 9. Implementation of Fuzzy control system on a 200MW SCPP for peak load generation

The SCPP equipped with 5 cm in thickness water bags cannot produce desired power in the desired period because a low heat capacity thermal storage cannot store sufficient thermal energy during day time. By increasing the thermal storage thickness to 10 cm (passive control) and implementing of the FLC system (active control), the SCPP tracks reference output power profile and can satisfy peak load demand in the grid. Consider that the behavior of the solar chimney power plant will completely change by the implementation of an FLC and appropriate thermal storage; Driving force (solar radiation) follower or day-generation solar power plant switches into night-time power generation plant. This fact shows the potential use of such simple and relatively cheap renewable power plants and appropriate control systems.

Finally, the inputs and output of the fuzzy logic controller in the peak load scenario for the 200MW SCPP equipped with 10 cm thermal storage thickness are shown in Fig. 10. In this case, suitable determination in scaling gains prevents the controller from being saturated too.

4. Conclusions

A semi-analytical mathematical model has been developed to investigate the time-dependent operation of an SCPP considering the aero-turbine and turbine inlet gate. The proposed model is validated in a reference un-controlled operation. In the following, a novel Fuzzy Logic Control (FLC) system is designed and Implemented on a large-scale solar chimney power plant equipped with artificial thermal energy storage (TES). Besides any passive control solution for an SCPP, active control by the mentioned FLC system makes the power plant more reliable and flexible to generate electrical power in the full range of grid demand from base load to peak load patterns. Results show that an integrated or hybrid control system comprises of FLC and TES system would be one of the best solutions for improvement in the time-depended performance of an SCPP techno-economically. Ease of development, functionality, reliability, and flexibility to meet the different requirements and conditions are some of the advantages of this novel control system. Further developments and optimizations of this proposed hybrid control system, can make an SCPP fully independent from environmental conditions, and help the large-scale SCPP technology to be commercialized.

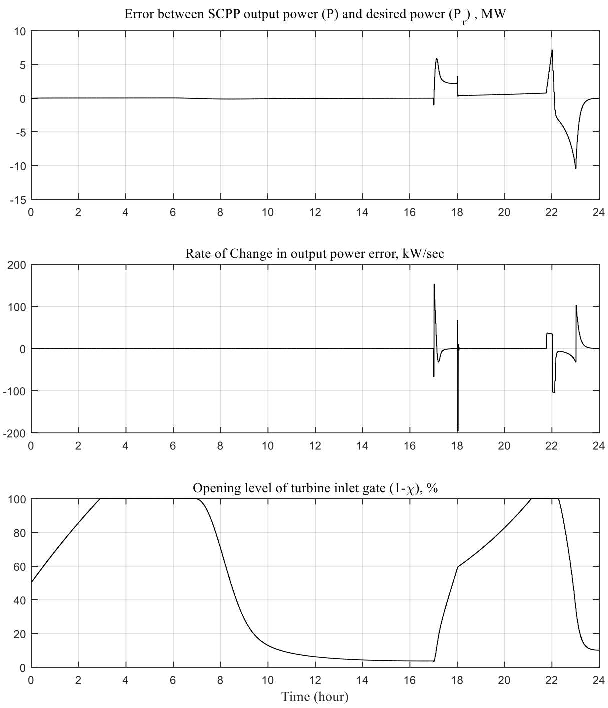

Figure 10. Values of FLC controller inputs and output in peak load scenario (Hs=10 cm)

Nomenclature

A_c	Collector area (m^2)
c	Rate of change in power generation error ($kW.s^{-1}$)
c_{pa}	Specific heat capacity of air ($J.Kg^{-1}.K^{-1}$)
c_s	Specific heat capacity of thermal storage ($J.Kg^{-1}.K^{-1}$)
D_h	Hydraulic diameter (m)
D_c	Collector diameter (m)
e	Error in power generation (MW)
f	Friction factor
g	Gravitational acceleration ($m.s^{-2}$)
G_h	Instantaneous global horizontal irradiation ($W.m^{-2}$)
h_i	Internal heat transfer coefficient in collector ($W.m^{-2}.K^{-1}$)
H_s	Effective thickness of ground or thermal storage (m)
H_t	Tower (chimney) height (m)
h_∞	Heat transfer coefficient from collector roof to ambient ($W.m^{-2}.K^{-1}$)
K	Minor loss coefficient
k	Thermal conductivity ($W.m^{-1}.K^{-1}$)
m_s	Effective mass of ground or thermal storage (kg)
$\dot{m}_a$	Mass flow rate of flowing air ($kg.s^{-1}$)
P	Instantaneous generated power (MW)
P_r	Reference power output (MW)
$\dot{Q}_a$	Volumetric flow rate ($m^3.s^{-1}$)
R_c	Collector radius (m)
R_t	Tower (chimney) radius (m)
T	Sampling interval time (s)

t	Time (s)
$\bar{T}_a$	Mean temperature of flowing air in collector (K)
$T_{a,i}$	Air temperature at collector inlet (K)
$T_{a,o}$	Air temperature at collector outlet (K)
T_s	Collector ground or thermal storage surface temperature (K)
T_∞	Ambient air temperature (K)
$\bar{u}_c$	Mean velocity of flowing (m.s^{-1})
u_{wind}	Ambient wind speed (m.s^{-1})
v_a	Mean updraft velocity in chimney (m.s^{-1})
Δp_{tot}	Total available pressure difference (Pa)
Δp_t	Aero turbine pressure drop (Pa)
Δp_g	Aero turbine inlet gate pressure drop (Pa)
Δp_l	Pressure drop due to losses (Pa)
Δp_d	Dynamic pressure change (Pa)

Greek symbols

α	Absorptivity of collector ground
η_{tg}	Turbo-generator efficiency
χ	Turbine inlet gate pressure drop coefficient
μ_a	Dynamic viscosity (kg.m^{-1}.s^{-1})
$\rho_{a,o}$	Density of air at chimney inlet (kg.m^{-3})
ρ_s	Density of ground (kg.m^{-3})
ρ_∞	Density of ambient air (kg.m^{-3})
τ	Transmissivity of collector roof
ξ	Total flow loss coefficient
ψ	Turbine pressure drop coefficient

References

1. Chen, C.J., *Physics of solar energy*. 2011: John Wiley & Sons.
2. Dhahri, A. and A. Omri, *A Review of solar Chimney Power Generation Technology*. International Journal of Engineering and Advanced Technology (IJEAT), 2013. **2**(3): p. 1-17.
3. Zhou, X., et al., *Special Climate around a Commercial Solar Chimney Power Plant*. Journal of Energy Engineering, 2008. **134**: p. 6-14.
4. Schlaich, J.r., et al. *Design of Commercial Solar Tower Systems: Utilization of Solar Induced Convective Flows for Power Generation*. in *ASME 2003 International Solar Energy Conference*. 2003. American Society of Mechanical Engineers.
5. dos Santos Bernardes, M.A., *Solar Chimney Power Plants-Developments and Advancements*. 2010: INTECH Open Access Publisher.
6. Padki, M. and S. Sherif, *On a simple analytical model for solar chimneys*. International Journal of Energy Research, 1999. **23**(4): p. 345-349.
7. Maia, C.B., et al., *Theoretical evaluation of the influence of geometric parameters and materials on the behavior of the airflow in a solar chimney*. Computers & Fluids, 2009. **38**(3): p. 625-636.
8. Gholamalizadeh, E. and S.H. Mansouri, *A comprehensive approach to design and improve a solar chimney power plant: A special case – Kerman project*. Applied Energy, 2013. **102**: p. 975-982.
9. Al-Dabbas, M.A., *The first pilot demonstration: solar updraft tower power plant in Jordan*. International Journal of Sustainable Energy, 2011: p. 1-12.
10. Zhou, X., et al., *Experimental study of temperature field in a solar chimney power setup*. Applied Thermal Engineering, 2007. **27**(11-12): p. 2044-2050.
11. Hurtado, F.J., A.S. Kaiser, and B. Zamora, *Evaluation of the influence of soil thermal inertia on the performance of a solar chimney power plant*. Energy, 2012. **47**(1): p. 213-224.
12. Koonsrisuk, A., S. Lorente, and A. Bejan, *Constructal solar chimney configuration*. International Journal of Heat and Mass Transfer, 2010. **53**(1-3): p. 327-333.
13. Bernardes, M.A.d.S. and T.W. von Backström, *Evaluation of operational control strategies applicable to solar chimney power plants*. Solar Energy, 2010. **84**(2): p. 277-288.

14. Ming, T., et al., *Numerical analysis of flow and heat transfer characteristics in solar chimney power plants with energy storage layer.* Energy Conversion and Management, 2008. **49**(10): p. 2872-2879.
15. Fluri, T.P. and T.W. Von Backström, *Performance analysis of the power conversion unit of a solar chimney power plant.* Solar Energy, 2008. **82**(11): p. 999-1008.
16. Tingzhen, M., et al., *Numerical simulation of the solar chimney power plant systems coupled with turbine.* Renewable Energy, 2008. **33**(5): p. 897-905.
17. Kebabsa, H., et al., *Thermo-hydrodynamic behavior of an innovative solar chimney.* Renewable Energy, 2020. **145**: p. 2074-2090.
18. Yaswanthkumar, A. and V. Chandramohan, *Numerical analysis of flow parameters on solar updraft tower (SUT) with and without thermal energy storage (TES) system.* Journal of Thermal Analysis and Calorimetry, 2019. **136**(1): p. 331-343.
19. Amudam, Y. and V.P. Chandramohan, *Influence of thermal energy storage system on flow and performance parameters of solar updraft tower power plant: A three dimensional numerical analysis.* Journal of Cleaner Production, 2019. **207**: p. 136-152.
20. Muhammed, H.A. and S.A. Atrooshi, *Modeling solar chimney for geometry optimization.* Renewable Energy, 2019. **138**: p. 212-223.
21. Mehla, N., K. Kumar, and M. Kumar, *Thermal analysis of solar updraft tower by using different absorbers with convergent chimney.* Environment, Development and Sustainability, 2019. **21**(3): p. 1251-1269.
22. Fallah, S.H. and M.S. Valipour, *Evaluation of solar chimney power plant performance: The effect of artificial roughness of collector.* Solar Energy, 2019. **188**: p. 175-184.
23. Das, P. and V. Chandramohan, *Effect of chimney height and collector roof angle on flow parameters of solar updraft tower (SUT) plant.* Journal of Thermal Analysis and Calorimetry, 2019. **136**(1): p. 133-145.
24. Das, P. and V.P. Chandramohan, *Computational study on the effect of collector cover inclination angle, absorber plate diameter and chimney height on flow and performance parameters of solar updraft tower (SUT) plant.* Energy, 2019. **172**: p. 366-379.
25. Cottam, P.J., et al., *Solar chimney power plants – Dimension matching for optimum performance.* Energy Conversion and Management, 2019. **194**: p. 112-123.
26. Bouabidi, A., et al., *Numerical analysis of chimney diameter effect on the fluid flow and the heat transfer characteristics within the solar tower.* Energy Sources, Part A: Recovery, Utilization, and Environmental Effects, 2019: p. 1-13.
27. Balijepalli, R., V. Chandramohan, and K. Kirankumar, *A complete design data and performance parameter evaluation of a pilot scale solar updraft tower.* Heat Transfer Engineering, 2019: p. 1-14.
28. Al-Kayiem, H.H., et al., *Performance evaluation of hybrid solar chimney for uninterrupted power generation.* Energy, 2019. **166**: p. 490-505.
29. Aurybi, M.A., et al., *Mathematical evaluation of solar chimney power plant collector, integrated with external heat source for non-interrupted power generation.* Sustainable Energy Technologies and Assessments, 2018. **30**: p. 59-67.
30. Zhou, X. and Y. Xu, *Pressure Losses in Solar Chimney Power Plant.* Journal of Solar Energy Engineering, 2018. **140**(2).
31. Xu, Y. and X. Zhou, *Performance of divergent-chimney solar power plants.* Solar Energy, 2018. **170**: p. 379-387.
32. Hassan, A., M. Ali, and A. Waqas, *Numerical investigation on performance of solar chimney power plant by varying collector slope and chimney diverging angle.* Energy, 2018. **142**: p. 411-425.
33. Toghraie, D., et al., *Effects of geometric parameters on the performance of solar chimney power plants.* Energy, 2018. **162**: p. 1052-1061.
34. Rabehi, R., et al., *Numerical simulation of solar chimney power plant adopting the fan model.* Renewable Energy, 2018. **126**: p. 1093-1101.
35. Djaouida, B., et al., *Controlling power output of solar chimney power plant according to demand.* International Journal of Ambient Energy, 2018: p. 1-15.
36. Pretorius, J.P., *Optimization and Control of a Large-scale Solar Chimney Power Plant*, in *Mechanical Engineering* 2007, University of Stellenbosch: Stellenbosch. p. 200.
37. Balijepalli, R., V.P. Chandramohan, and K. Kirankumar, *Optimized design and performance parameters for wind turbine blades of a solar updraft tower (SUT) plant using theories of Schmitz and aerodynamics forces.* Sustainable

Energy Technologies and Assessments, 2018. **30**: p. 192-200.
38. Ayadi, A., et al., *Unsteady state of a solar chimney power plant accoupled with a turbine: case study*. 2018. **16**(2): p. 244-255.
39. Zhou, X., Y. Xu, and Y. Hou, *Effect of Flow Area to Fluid Power and Turbine Pressure Drop Factor of Solar Chimney Power Plants.* Journal of Solar Energy Engineering, 2017. **139**(4).
40. Ming, T., et al., *Solar updraft power plant system: A brief review and a case study on a new system with radial partition walls in its collector.* Renewable and Sustainable Energy Reviews, 2017. **69**: p. 472-487.
41. Li, J., H. Guo, and S. Huang, *Power generation quality analysis and geometric optimization for solar chimney power plants.* Solar Energy, 2016. **139**: p. 228-237.
42. Guo, P., et al., *Evaluation of the optimal turbine pressure drop ratio for a solar chimney power plant.* Energy Conversion and Management, 2016. **108**: p. 14-22.
43. Choi, Y.J., et al., *Development of analytical model for solar chimney power plant with and without water storage system.* Energy, 2016. **112**: p. 200-207.
44. Chaichan, M.T. and H.A. Kazem, *Thermal Storage Comparison for Variable Basement Kinds of a Solar Chimney Prototype in Baghdad - Iraq Weathers.* International Journal of Applied Sciences (IJAS), 2011. **2**(2): p. 12-20.
45. G.M.Ngala, A.T. Sulaiman, and I. Garba, *Review of Solar Chimney Power Technology and Its Potentials in Semi-Arid Region of Nigeria.* International Journal of Modern Engineering Research (IJMER), 2013. **3**(3): p. 1283-1289.
46. Ali, M.H., *Analysis Study of Solar Tower Power Plant & Its Configuration Effects on Its Performance in Iraq (Baghdad City).* Modern Applied Science, 2013. **7**(4): p. 55.
47. Passino, K.M., *Intelligent control: an overview of techniques*. 2001, New York: IEEE Press. p. 104-133.
48. Jager, R., *Fuzzy Logic in Control*. 1995, TU Delft, Delft University of Technology.
49. Stirrup, R. and A.J. Chipperfield, *Highly nonlinear control of a solar thermal power plant using soft computing fuzzy tuning techniques.* ISES Solar World Congress 2003, 2003.
50. Luk, P., K. Low, and A. Sayiah, *GA-based fuzzy logic control of a solar power plant using distributed collector fields.* Renewable energy, 1999. **16**(1): p. 765-768.
51. Rubio, F.R., M. Berenguel, and E.F. Camacho, *Fuzzy logic control of a solar power plant.* Fuzzy Systems, IEEE Transactions on, 1995. **3**(4): p. 459-468.
52. Usta, M., O. Akyaszi, and I. Atlas. *Design and performance of solar tracking system with fuzzy logic Controller*. in *Sixth International Advanced Technologies Symposium (IATS'11), Elazig, Turkey, May16-18*. 2011.
53. Siddik, A. and M. Shangeetha, *Implementation of Fuzzy Logic controller in Photovoltaic Power generation using Boost Converter and Boost Inverter.* International Journal of Power Electronics and Drive Systems (IJPEDS), 2012. **2**(3): p. 249-256.
54. Cheikh, M.A., et al., *Maximum power point tracking using a fuzzy logic control scheme.* Revue des energies Renouvelables, 2007. **10**(3): p. 387-395.
55. Hamed, B.M. and M.S. El-Moghany, *Fuzzy controller design using FPGA for sun tracking in solar array system.* International Journal of Intelligent Systems and Applications (IJISA), 2012. **4**(1): p. 46.
56. Simoes, M.G. and N. Franceschetti. *Fuzzy optimisation based control of a solar array system*. in *Electric Power Applications, IEE Proceedings-*. 1999. IET.
57. Pretorius, J.P. and D.G. Kröger, *Critical evaluation of solar chimney power plant performance.* Solar Energy, 2006. **80**(5): p. 535-544.
58. Aurélio dos Santos Bernardes, M., T.W. Von Backström, and D.G. Kröger, *Analysis of some available heat transfer coefficients applicable to solar chimney power plant collectors.* Solar Energy, 2009. **83**(2): p. 264-275.
59. Bernardes, M.A.D.S., *Convective Heat Transfer Analysis of Solar Chimney Power Plant Collectors*, in *Heat Transfer - Mathematical Modelling, Numerical Methods and Information Technology*, A. Belmiloudi, Editor. 2011, InTech.
60. Passino, K.M., S. Yurkovich, and M. Reinfrank, *Fuzzy control*. Vol. 42. 1998: Citeseer.
61. Zhou, X., F. Wang, and R.M. Ochieng, *A review of solar chimney power technology.* Renewable and Sustainable Energy Reviews, 2010. **14**(8): p. 2315-2338.